



GSJ: Volume 9, Issue 8, August 2021, Online: ISSN 2320-9186

www.globalscientificjournal.com

MODELING EFFECT OF STEAM TO METHANE RATIO IN THE PERFORMANCE OF AMMONIA PRODUCTION

UCHE Bethel Chikeziri, Ehirim, E.O., Wordu, A.A.

Department of Chemical/Petrochemical Engineering, Rives State University, Nkpolu-Oroworukwu, Port Harcourt, Nigeria

Email: Bethyblack4sure@gmail.com

Abstract

Steam methane reforming is a chemical synthesis for producing syngas (hydrogen and carbon monoxide) from hydrocarbon such as natural gas and is mostly used in ammonia production. To ensure optimal efficiency, the ratio of steam and methane should be high to obtain more of hydrogen needed for ammonia production. A detailed mathematical models were developed for steam reforming by applying the principle of conservation of mass and energy, the model equations were integrated numerically using the 4th order Runge- Kulta algorithm. Simulation of functional parameters was performed using Aspen Hysys. The model predictions shows a percentage derivation of 0.019% minimum and 8.7% maximum, which depict that the model results were in agreement with literature data. The effect of steam to methane ratio on the primary reformer was studied and the result was compared to literature plant data in other to test the validity of the model. From the result the conversion of methane was dependent on the operating condition such as temperature and pressure and inlet composition. The result showed that as the steam to methane ratio increases there is a slight increment in the conversion of methane which had a huge effect on the amount of hydrogen produced for ammonia production. This worked showed clearly that ammonia production was favoured by high steam to gas ratio.

Key Words: Ammonia, Methane, Steam reforming, Model, Mass, Energy

1. Introduction

Ammonia is a colorless, pungent, suffocating, highly water soluble gaseous compound usually produced by the direct combination of nitrogen and hydrogen gases, used chiefly for refrigeration and in the manufacturing of commercial chemical and laboratory reagent. Ammonia is crucial in the manufacturing of fertilizer, and is one of the volume synthetic chemicals produced in the world.

1.1 Process Description

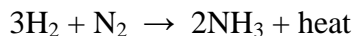
The inlet temperature at the normal operating conditions is 320°C. The process gas is heated to this temperature partly by passing through a feed/effluent/gas exchanger, E 3311, and partly through E 3209, a trim heater. The for seen gas composition will have a temperature increase of 18-19°C corresponding to an outlet temperature of 339°C. The gas/gas exchanger, E 3311, cools the purification of gas to 92°C. To remove as much water as possible from the purified gas, it is further cooled to 38°C by the final gas cooler, E 3312. The condensate is separated from the purified gas in the final gas separator, B 3311.

The purified gas outlet, B 3311, contains N₂, H₂ and approximately 1 mol% of inert as Ar, CH₄ and H₂O. The ratio of H₂ to N₂ is approximately 3:1.

1.2 Ammonia Synthesis Section

General Process Description

The ammonia synthesis takes place in the ammonia synthesis converter, R 3501, according to the following reaction scheme:



The reaction is reversible and only a part of the hydrogen and nitrogen is converted into ammonia by passing through the catalyst bed. The conversion of the equilibrium concentration of ammonia is favored by high pressure and low temperature. In R 3501 only about 30% of the nitrogen and the hydrogen are converted into ammonia. To get maximum overall yield of the synthesis gas, the unconverted part will be recycle to the converter after separation of the liquid ammonia product.

After the synthesis gas has passed through R 3501, the effluent gas will be cooled down to a temperature which the main part of the ammonia is converted.

The circulation is carried out by means of the re-circulator, which is an integrated part of the synthesis compressor, K 3431.

As the reaction rate is very much enhanced by high temperature, the choice of temperature is based on a compromise between the theoretical conversion and the approach to equilibrium.

The ammonia synthesis loop has been designed for a maximum pressure of 245kg/cm² g. The normal operating pressure will be 220kg/cm² g depending on load and catalyst activity.

The normal operating temperatures will be in range of 360-525°C for the 1st bed and 370-460°C for the 2nd bed.

The heat liberated by the reaction (about 750kcal/kg produced ammonia) is utilized for high pressure steam production (in the loop waste heat boiler, E 3501) and preheat of high pressure boiler feed water.

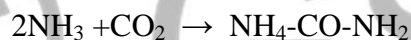
As illustrated in diagram, the converted effluent gas is cooled stepwise, first in the loop waste heat boiler, E 3501, from 456-350°C. Next step is cooling to about 269°C in the boiler feed water

preheated, E3502. And then the hot heat exchanger, E 3503, where the synthesis effluent gas is cooled to 61°C by preheating of converter feed gas.

The synthesis gas is cooled to 37°C in the water cooler, E 3504 and to 28°C in the heat exchanger.

The final cooling to 12°C takes place in the ammonia chillers. The condensed ammonia is separated from the circulated to the ammonia converter through the cold heat exchanger, the recirculator, and the hot heat exchanger.

The water vapour concentration in the make-up gas is in the range of 200-300 ppm, depending on the operating pressure in the loop. The water is removed by absorption in the condensed ammonia. The carbon dioxide in the make-up gas will react with both gaseous and liquid ammonia, forming ammonium carbonate:



The formed carbamate is dissolved in the condensed ammonia. As the water deactivates the ammonia synthesis catalyst, the content of carbon monoxide in the make-up synthesis gas should be kept as low as possible. Inert Gases

The make-up gas enters the loop between the two ammonia chillers. This gas contains small amount of argon and methane. These gases are inert in the sense that they pass through the synthesis converter without undergoing any chemical changes. The inert will accumulate in the synthesis loop, and a high inert level, i.e. high concentration of inert gases will build up in the circulating synthesis gas. The inert level will increase until the addition of inert gases will make the makeup gas in the same as the amount of inert removed from the top.

The low temperature outlet of the 1st ammonia chiller means that the partial pressure of ammonia in the gas phase is relatively low. Only a minor amount of ammonia will be removed together with the purge gas. The purge gas is further cooled in the purge gas chiller, E 3511, and the liquid ammonia is separated in B 3512. The liquid ammonia is sent to B3501. Approximately 98% of ammonia is currently produced with natural gas as feedstock using steam shifting, though a minority obtain hydrogen from coal or through the catalytic reforming of naphtha. Interestingly, as hydrogen is mixed with air at the start of the reaction, many molecules of atmospheric oxygen react with hydrogen to form water, removing the oxygen gas which comprises 21% of air.

1.3 Hydrogen/Nitrogen Ratio

By the synthesis reaction, 3 volumes of hydrogen reacts with 1 volume of nitrogen to form 2 volumes of ammonia. The synthesis loop is designed for operating at H_2/N_2 ratio of 3.0, but special conditions may make it favorable to operate at a slightly different ratio in the range of 2.5-3.5. When the ratio is decreased to 2.5, the reaction rate will increase slightly, but decrease again for ratios below 2.5. On the other hand the circulating synthesis gas will be heavier. Therefore, the pressure drop and ammonia concentration at the inlet of the ammonia synthesis converter will increase.

1.4 Ammonia Converter

At the top of the converter, the gas passes the tube side of the inter bed heat exchanger, where the inlet gas is heated up to the reaction temperature of the heated up the reaction temperature of the 1st catalyst bed by the heat exchanger with gas leaving the 1st catalyst bed. The gas inlet

temperature to the 1st bed is adjusted by means of the so-called “cold shots” which is cold synthesis gas introduced through the transfer pipe of the center tube.

The gas, which leaves the 1st catalyst bed, is led through the 2nd bed and into the center tube from which it is returned to the ammonia loop.

The two catalyst bed contains a total of 109.3 m³ of KMIR catalyst, which is a promoted iron catalyst containing small amounts of non-reducible oxides.

1.5 Reaction Temperature

At the inlet of R 3501, 1st catalyst bed, the minimum temperature of approx. 360°C is required to ensure a sufficient reaction rate. If the temperature at the catalyst inlet is below this value, the reaction rate will become so low that the heat liberated by the reaction becomes too small to maintain the temperature in the converter (Schmitkey, Gary 2014). The reaction will quickly extinguish itself if properly adjustments are not made immediately.

On the other hand, it is desirable to keep the catalyst temperature as low as possible to prolong the catalyst life. Therefore, it is recommended to keep the catalyst inlet temperature slightly above the minimum temperature. It is anticipated that the synthesis gas enters the 1st catalyst bed at a temperature of max. 400°C. As the gas passes through the catalyst bed the temperature increases to a maximum temperature in the outlet from the 1st bed, which is normally the highest temperature in the converter, called the “hot spot”. The temperature of the hot spot is upto 510°C, but should not exceed 520°C. The gas from the 1st bed is cooled with some of the cold inlet gas to the 1st bed in order to obtain a temperature of approx. 370°C inlet 2nd bed. The gas outlet temperature from the 2nd bed is about 455°C.

2. Materials and Methods

2.1 Materials

The research adopts analytical techniques. The materials component to accomplish the research is:

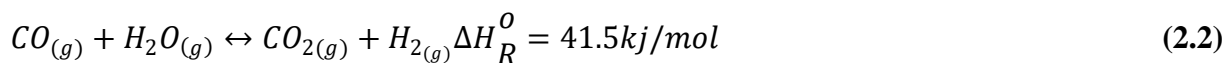
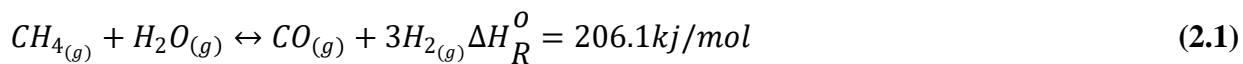
- i. Materials and Energy Balance.
- ii. Appropriate Kinetic model literature.
- iii. Thermodynamics principle and data.
- iv. Model simulation computer package (matlab and aspen hysys).
- v. Feed composition.
- vi. Process flow diagram for inlet and outlet component.

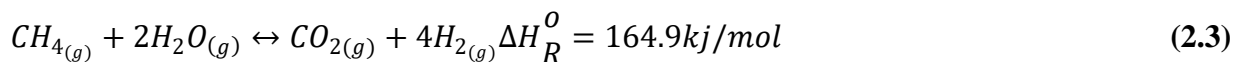
2.2 Methods

The methods used in this work are as follows:

2.2.1 Steam Methane Reforming Kinetic Model

Xu and Froment (1989) Investment steam methane reforming over NilmgA1204 catalyst in a tubular reaction. There result shows that three main reactions should be consider in other to have a whole aspect of the process defining the specific rate equations based on Langmuir Hinshe wood mechanism.





The associated rate as proposed by Xu and Froment (1989) can be written as follows:

$$r_1 = \frac{\frac{K_1}{P^{2.5}H_2} \left((PCH_4 \cdot PH_2O - \frac{P^3 H_2 \cdot PCO}{K_{e,1}}) \right)}{(DEN)^2} \quad (2.4)$$

$$r_2 = \frac{\frac{K_2}{PH_2} \left((PCO \cdot PH_2O - \frac{PH_2 \cdot PCO_2}{K_{e,2}}) \right)}{(DEN)^2} \quad (2.5)$$

$$r_3 = \frac{\frac{K_3}{P^3 H_2} \left((PCH_4 \cdot PH_2O - \frac{P^4 H_2 \cdot PCO}{K_{e,3}}) \right)}{(DEN)^2} \quad (2.6)$$

$$DEN = 1 + K_{CO} \cdot PCO + K_{CH_4} + KH_2O * \frac{PH_2O}{PH_2} \quad (2.7)$$

In terms of mole fractions the rate expression can be written as:

$$P_j \cdot y_j = P \quad (2.8)$$

Substituting (3.8) for the partial pressure in the rate equation we obtain:

$$r_1 = \frac{\frac{K_1}{P^{2.5}H_2 * P^{0.5}} \left((yCH_4 \cdot yH_2O - \frac{P^3 y^3 H_2 \cdot yCO}{K_{e,1}}) \right)}{(DEN)^2} \quad (2.9)$$

$$r_2 = \frac{\frac{K_2 \cdot P}{yH_2} \left((yCO \cdot yH_2O - \frac{yH_2 \cdot yCO_2}{K_{e,2}}) \right)}{(DEN)^2} \quad (2.10)$$

$$r_3 = \frac{\frac{K_3}{y^{3.5}H_2 \cdot P^{0.5}} \left((yCH_4 \cdot y^2 H_2O - \frac{P^2 y^4 H_2 \cdot yCO}{K_{e,3}}) \right)}{(DEN)^2} \quad (2.11)$$

$$DEN = 1 + P \cdot (K_{CO} \cdot y_{CO} + K_{H_2} + y_{H_2} K_{CH_4} \cdot y_{CH_4}) + K_{H_2O} X \frac{y_{H_2O}}{y_{H_2}} \quad (2.12)$$

Where;

K_i :	Rate Constant for reaction i
$K_{e,i}$	Equilibrium Constant for reaction i
K_j	Adsorption Constant for component j
P_j	partial Pressure for Component j

The dependences on temperature of kinetic rates constants, K_2 , adsorption parameters, K_j were expressed.

The pre-exponential factors for $K_{i,0}$ and $K_{j,0}$, activation energy for reaction i, E_i and the enthalpy of adsorption for component $j \Delta H_j$ were determined by Arrhenius equation and Van't Hopp equation.

i : for reactions

j : for reaction components of species

$$K_i = K_{i,0} \exp \left[\frac{E_i}{R} \left(\frac{1}{T_r} - \frac{1}{T} \right) \right] \quad (2.13)$$

$$K_j = K_{j,0} \exp \left[\frac{\Delta H_j}{R} \left(\frac{1}{T_r} - \frac{1}{T} \right) \right] \quad (2.14)$$

$$K_{e,i} = \exp \left(\frac{\Delta_i G^0}{RT} \right) \quad (2.15)$$

$$G_j^0 = \Delta A_j + \Delta B_j \cdot T + \Delta C_j \cdot T^2 \quad (2.16)$$

2.2.2 Ammonia Synthesis Kinetic Model

The most widely used rate expression for ammonia synthesis as the Tenkin – Pyzhev equation, was first proposed in 1940 (citation).

The Tenkin – Pyzhev equation has been used successfully by various investigators to fit experimental data for both ammonia synthesis and ammonia decomposition.

The heart of this equation is the replacement of the Langmuir isotherm for nitrogen by a Frukin Isotherm which assumes a heat of adsorption which changes linearly with coverage.

For the overall reaction for ammonia synthesis, they proposed by:



2.2.3 Mass Balance

A packed bed reactor is a cylindrical tube which consists of an immobilized bed of catalyst.

Figure 3.1 shows the geometry of a packed bed reactor, the inlet parameter and the outlet parameter. If an infinitesimal section or control volume of the reactor is considered and a material balance is taken about the volume, the mass balance model will be established

Taking component balance about the control volume:

$$\left[\begin{array}{l} \text{Rate of infow} \\ \text{of component } j \\ \text{into volume} \\ \text{element per time} \end{array} \right] = \left[\begin{array}{l} \text{Rate of infow} \\ \text{of component } j \\ \text{into volume} \\ \text{element per time} \end{array} \right] - \left[\begin{array}{l} \text{Rate of outfow} \\ \text{of component } j \\ \text{from volume element} \\ \text{per time} \end{array} \right] + \left[\begin{array}{l} \text{Rate of generation} \\ \text{of component } j \\ \text{within volume} \\ \text{element per time} \end{array} \right] \quad (2.18)$$

In this model, the following assumptions will be made:

- i. Steady state operation
- ii. Axial and radial dispersions are negligible
- iii. Inter-phase mass resistance is negligible
- iv. Radial velocity gradient is neglected

$$\left[\begin{array}{l} \text{Rate of accumulation} \\ \text{of component } j \\ \text{within element volume} \\ \text{per time in mols/time} \end{array} \right] = \frac{dN_j}{dt} = 0 \quad (2.19)$$

$$\left[\begin{array}{l} \text{Rate of infow of} \\ \text{component } j \text{ into volume} \\ \text{element per time} \\ \text{in mols/time} \end{array} \right] = F_j I_z \quad (2.20)$$

$$\left[\begin{array}{l} \text{Rate of infow of} \\ \text{component } j \text{ into} \\ \text{volume element per} \\ \text{time in mols/time} \end{array} \right] = F_j I_{z+\Delta z} \quad (2.21)$$

$$\left[\begin{array}{l} \text{Rate of generation} \\ \text{of component } j \\ \text{within volume element} \\ \text{per time in mols/time} \end{array} \right] = P_B (\sum_i j v_i \cdot j r_i) \Delta V \quad (2.22)$$

Substituting equations (3.24), (3.25), (3.26) in equation (3.23), we have:

$$F_j I_z - F_j I_{z+\Delta z} + P_B (\sum_i j v_{i,j} \eta_i r_i) \Delta V = 0 \quad (2.23)$$

$$-F_j I_z - F_j I_{z+\Delta z} + P_B (\sum_i j v_{i,j} \eta_i r_i) \Delta V = 0 \quad (2.24)$$

$$\Delta V = A_c \cdot \Delta l \quad (2.25)$$

Substituting equation (3.30) in (3.29), we obtain:

$$-F_j I_z - F_j I_{z+\Delta z} + P_B (\sum_i j v_{i,j} \eta_i r_i) \Delta V = A_c \cdot \Delta l = 0 \quad (2.26)$$

Dividing through by Δl and taking limit as $\Delta l \rightarrow 0$, we have:

$$-\frac{dF_j}{dl} + P_B A_c (\sum_i j v_{i,j} \eta_i r_i) = 0 \quad (2.27)$$

$$\frac{dF_j}{dl} + P_B A_c (\sum_i, j V_{i,j} \eta_i r_i) \quad (2.28)$$

Equation (3.28) is the one dimensional steady mole for a packed bed reactor.

With respect to dimensionless length z

$$Z = \frac{l}{IR} \Rightarrow dl = IR dz \quad (2.29)$$

Equation (3.28) becomes

$$\frac{dF}{dz} + P_B I_R (\sum_i, j V_{i,j} \eta_i r_i) \quad (2.30)$$

Considering the reaction rates, the mass balance with respect to the reactant and product species are written as:

J: component (CH_4, H_2O, CO, H_2, N_2)

$$\frac{dF}{dz} + P_B \cdot A_c \sum (\eta_i r_i)$$

For Methane

$$\begin{aligned} \frac{dF_{CH_4}}{dz} &= P_B \cdot A_c \cdot I_R (-\eta_i r_i - \eta_3 r_3) \\ &= -P_B \cdot A_c \cdot I_R (\eta_i r_i + \eta_3 r_3) \end{aligned} \quad (2.31)$$

For Steam

$$\begin{aligned} \frac{dF_{H_2O}}{dz} &= P_B \cdot A_c \cdot I_R (-\eta_i r_i - \eta_2 r_2 - \eta_3 r_3) \\ &= -P_B \cdot A_c \cdot I_R (\eta_i r_i + \eta_2 r_2 + \eta_3 r_3) \end{aligned} \quad (2.32)$$

For Carbon Monoxide

$$\frac{dFCO}{dz} = P_B \cdot A_c \cdot I_R (\eta_1 r_1 - \eta_2 r_2) \quad (2.33)$$

For Carbondioxide

$$\frac{dFCO_2}{dz} = P_B \cdot A_c \cdot I_R (\eta_1 r_1 + \eta_3 r_3) \quad (2.34)$$

For Hydrogen

$$\frac{dFH_2}{dz} = P_B \cdot A_c \cdot I_R (3\eta_1 r_1 + \eta_2 r_2 + 4\eta_3 r_3 - 3\eta_4 r_4) \quad (2.35)$$

For Nitrogen

$$\frac{dFN_2}{dz} = P_B \cdot A_c \cdot I_R (\eta_4 r_4) \quad (2.36)$$

2.2.4 Energy Balance

Isothermal condition are most useful for the measurement of kinetic data. Real reactor operations are normally non-isothermal with limits of heat exchange, the reactor can operate isothermally (maximum heat exchange), adiabatically (no heat exchange) or non-isothermal regime (some extent of heat exchange). These three types of reactor operations yield different profits with the reactor.

In the energy balance model, the following assumption will be made:

- i. Kinetic energy change are negligible compared to those in the internal energy.
- ii. Potential energy change are negligible compared to those in the internal energy.
- iii. Negligible shaft work
- iv. Steady state operation

Taking energy balance about the control volume we obtain:

$$\left[\begin{array}{c} \text{Rate of energy} \\ \text{Input} \end{array} \right] - \left[\begin{array}{c} \text{Rate of energy} \\ \text{output} \end{array} \right] + \left[\begin{array}{c} \text{Rate of} \\ \text{Generation of energy} \end{array} \right] = \left[\begin{array}{c} \text{Rate of Accumulation} \\ \text{of energy} \end{array} \right] \quad (2.37)$$

$$\left[\begin{array}{c} \text{Rate of energy} \\ \text{Input} \end{array} \right] = \left[\begin{array}{c} \text{Rate of energy} \\ \text{input by flow} \\ \text{by flow of material} \end{array} \right] + \left[\begin{array}{c} \text{Rate of heat} \\ \text{addition by} \\ \text{the surroundings} \end{array} \right] \quad (3.38)$$

$$\left[\begin{array}{c} \text{Rate of energy} \\ \text{output} \end{array} \right] = \left[\begin{array}{c} \text{Rate of energy output} \\ \text{by flow of material} \end{array} \right] \quad (2.39)$$

$$\left[\begin{array}{c} \text{Rate of Accumulation} \\ \text{of energy} \end{array} \right] = \frac{dH_j}{dt} = 0 \quad (2.40)$$

$$\left[\begin{array}{c} \text{Rate of energy} \\ \text{Input} \end{array} \right] = \sum_j F_j \cdot H_j I_v \quad (2.41)$$

$$\left[\begin{array}{c} \text{Rate of energy} \\ \text{output} \end{array} \right] = \sum_j F_j \cdot H_j I_{v+\Delta v} \quad (2.42)$$

$$\left[\begin{array}{c} \text{Rate of generation of} \\ \text{energy} \end{array} \right] = P_B \sum_j (\Delta H_R, i) \cdot v_j \eta_i r_i \Delta v \quad (2.43)$$

$$\sum_j F_j \cdot H_j I_{v+\Delta v} + P_c \sum_{i,j} ((\Delta H_R, i) \cdot v_j \eta_i r_i) \Delta v = 0 \quad (2.44)$$

$$\sum_j F_j \cdot H_j I_v = \sum_j F_j \cdot H_j \quad (2.45)$$

$$\sum_j F_j \cdot H_j I_{v+\Delta v} = \sum_j [F_j \cdot H_j + d(F_j \cdot H_j)] \quad (2.46)$$

$$\text{RHS} = \sum [F_j \cdot H_j + dH_j + H_i dF_j] \quad (2.47)$$

$$H_j = Cp_j (T - T_r) \quad (2.48)$$

$$dH_j = Cp_j dT \tag{2.49}$$

Substituting equation (3.55), (3.57), (3.58) and (3.59) into (3.54), we have:

$$-\sum_j F_j \cdot Cp_j dT - \sum_j Cp_j (T - T_r) + P_B \cdot \sum_{i,j} \left((\Delta H_{R,i}) \cdot v_{i,j} \eta_i r_i \right) \Delta v + dp = 0 \tag{3.60}$$

Divide through by dv and simplify we have:

$$-\sum_j F_j \cdot Cp \frac{dT}{dv} - \sum_j Cp_j (T - T_r) + P_B \cdot \sum_{i,j} \left((\Delta H_{R,i}) \cdot v_{i,j} \eta_i r_i \right) \frac{dQ}{dv} = 0 \tag{2.50}$$

$$dp = U \cdot \pi D \cdot dz (T_w - T) \tag{2.51}$$

$$dv = AL = AL_R \cdot dz = \pi D^2 \cdot dz \tag{2.52}$$

$$-\sum_j F_j \cdot Cp \frac{dT}{dv} - \sum_j Cp_j \frac{dF}{dv} (T - T_r) + P_B \cdot \sum_{i,j} \left((\Delta H_{R,i}) \cdot v_{i,j} \eta_i r_i \right) + \frac{U \pi D \cdot dz (T_w - T)}{\pi D^2 \cdot dz} = 0 \tag{3.64}$$

3. Results and Discursion

The effect of steam to methane gas ratio indicates that methane (CH₄) and steam gases are species introduced into the system as inlet gases. Hence the ratio of steam to methane gas is an important parameter since it defines the inlet flow condition. The flow of methane is a constant in own model therefore an increase in the ratio of steam to methane implies a corresponding increase in flow of steam in the primary reformed as shown below.

$$\phi_{H_2O} = \frac{FH_{2,0}}{FCH_{4,0}}$$

Table 4.1 Comparisons between plant data and model predictions at the primary reformer exit.

Property	Plant	Model prediction	Percentage error %
Flue gas temperature	1030	940	8.7

Flue gas flow rate	8195.31	8191	0.52
Process gas temperature	784	780	0.51
Process gas pressure	32	30.8	3.8
Dry gas flow rate	4219.82	4139.02	0.019
Steam\dry gas	0.86	0.88	2.3

Figure 4.1 illustrates the plot showing the effect of high steam ratio in the primary reform for a steam to gas ratio of 3.0. It can be observed from the graph that methane has the highest fractional conversion. After about 15% of the reaction, the fractional conversion almost became independent of the reactor length. About 10% of the reactor length both the methane and carbon dioxide fractional conversion attained the maximum point. However, the carbon dioxide fractional conversion assumes a sharp decrease along the reactor length to almost zero at the end of the reactor. The nitrogen fractional conversion remains practically unaltered along the whole reactor length. This is because the nitrogen did not take part in any chemical reaction in the reactor. This behavior is also true when the steam to gas ratio is 3.5 and 4.0 as shown in figure 4.2 and 4.3 respectively.

Figure 4.3 which shows that the fractional conversion against the dimension reactor length for a steam to gas of 4.0. This graph shows that the methane conversion was on the increase. This also indicates the production of hydrogen and ammonia in the secondary reformer will be favoured with an increase in the steam to gas ratio of 4.0.

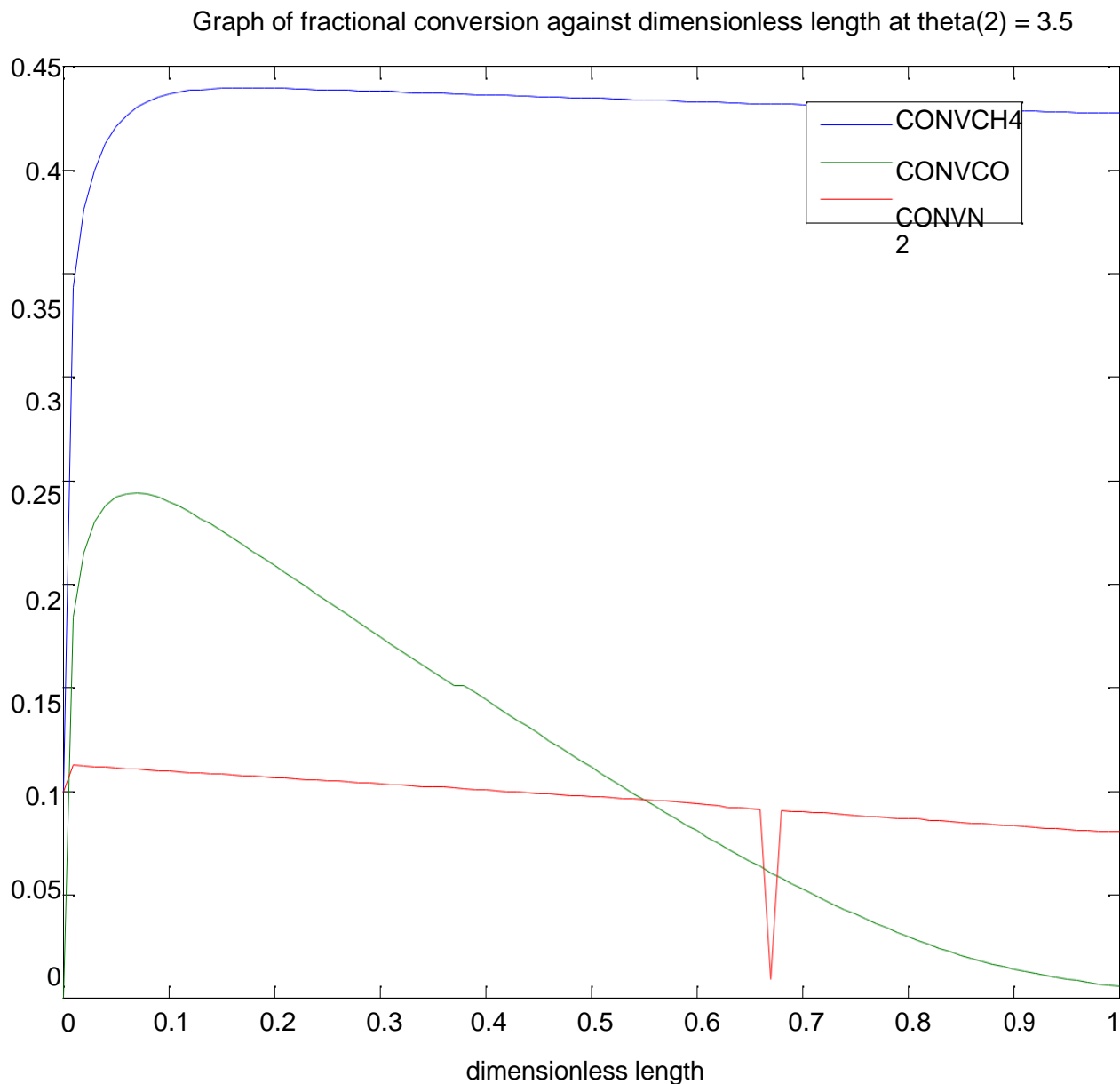


Figure 4.1: Fractional conversion against dimensionless reactor length for a steam to gas ratio of 3.0

It can clearly be observed that the fractional conversion of nitrogen remain constant in all the cases simulated in the primary reformer. The major conversion took place in the inlet of the reactor. The fractional conversion of carbondioxide fall close to zero at the outlet of the reactor in all the cases simulated.

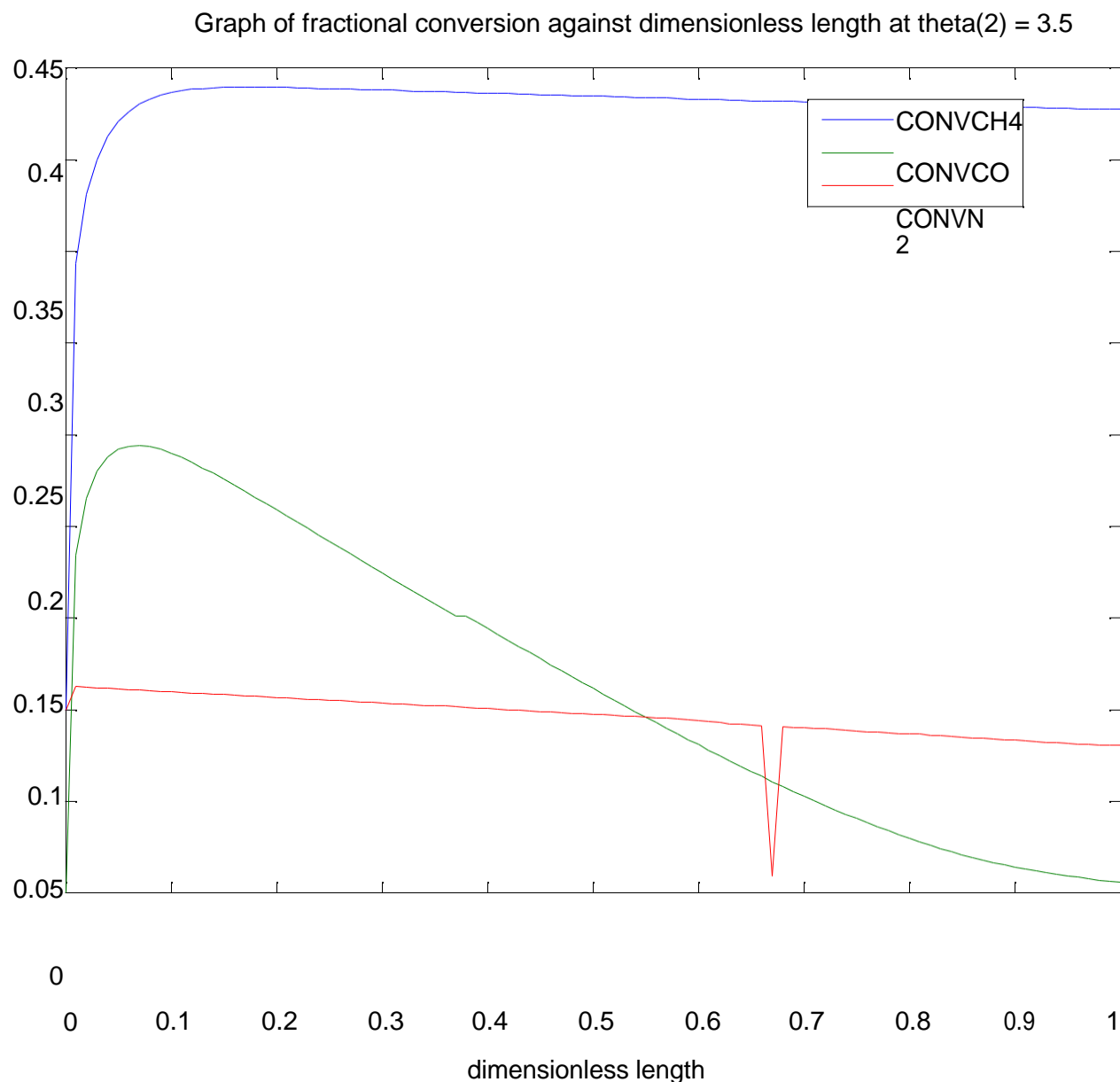


Figure 4.2: Fractional conversion against dimensionless reactor length for a steam to gas ratio of 3.5

Figure 4.2 which shows that the fractional conversion against the dimension reactor length for a steam to gas of 3.5 This plot shows that the methane conversion was on the increase. This also indicate that fractional conversion of carbondioxide fall close to zero at the outlet of the reactor in all the cases simulated.

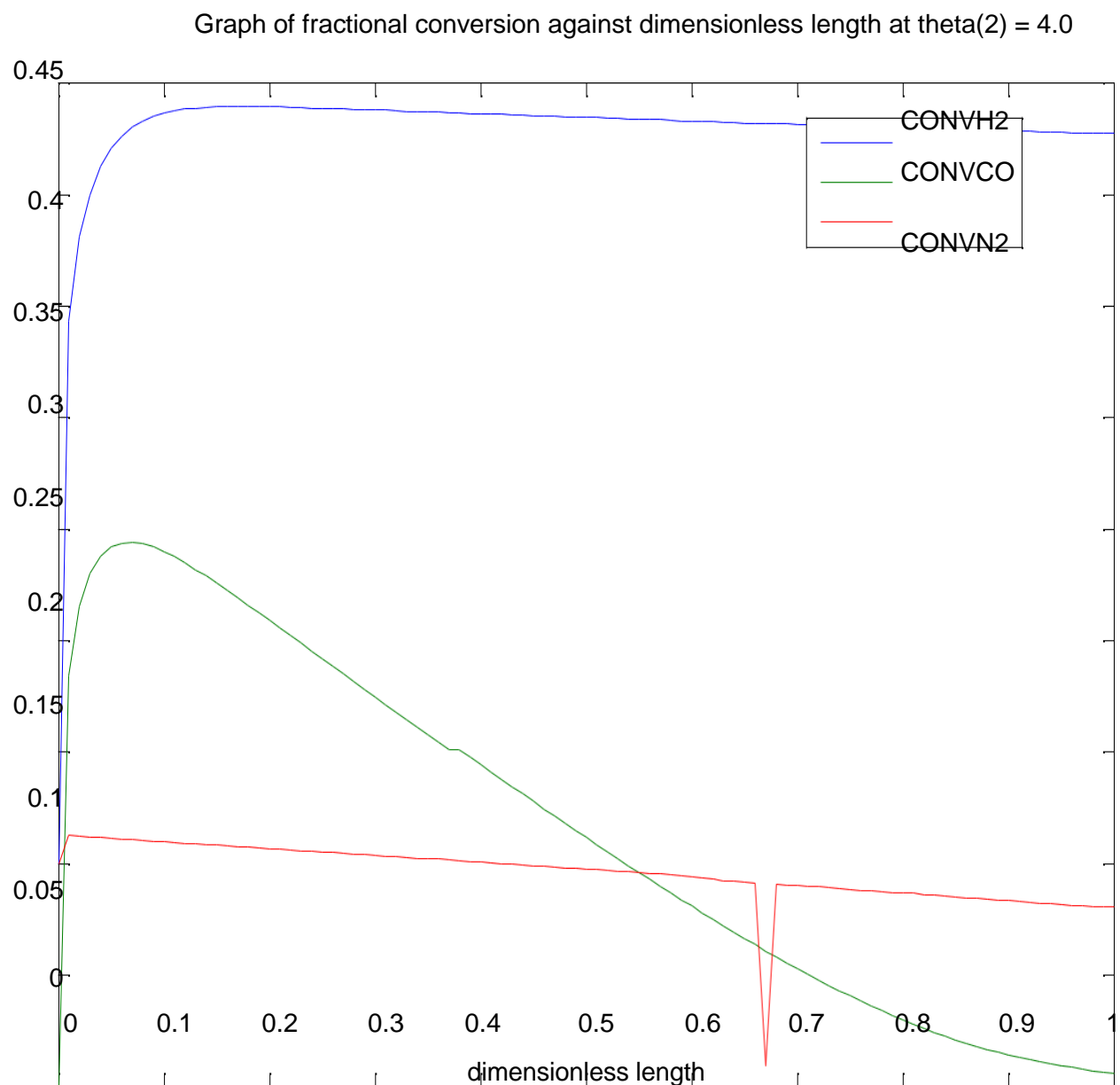


Figure 4.3: Fractional conversion against dimensionless reactor length for a steam to gas ratio of 4.0

Figure 4.3 shows that the fractional conversion against the dimension reactor length for a steam to gas of 4.0. This graph shows that the methane conversion was on the increase. This also indicates

the production of hydrogen and ammonia in the secondary reform will be favoured with an increase in the steam to gas ratio of 4.

Simulation of the plant using hysys v8.6

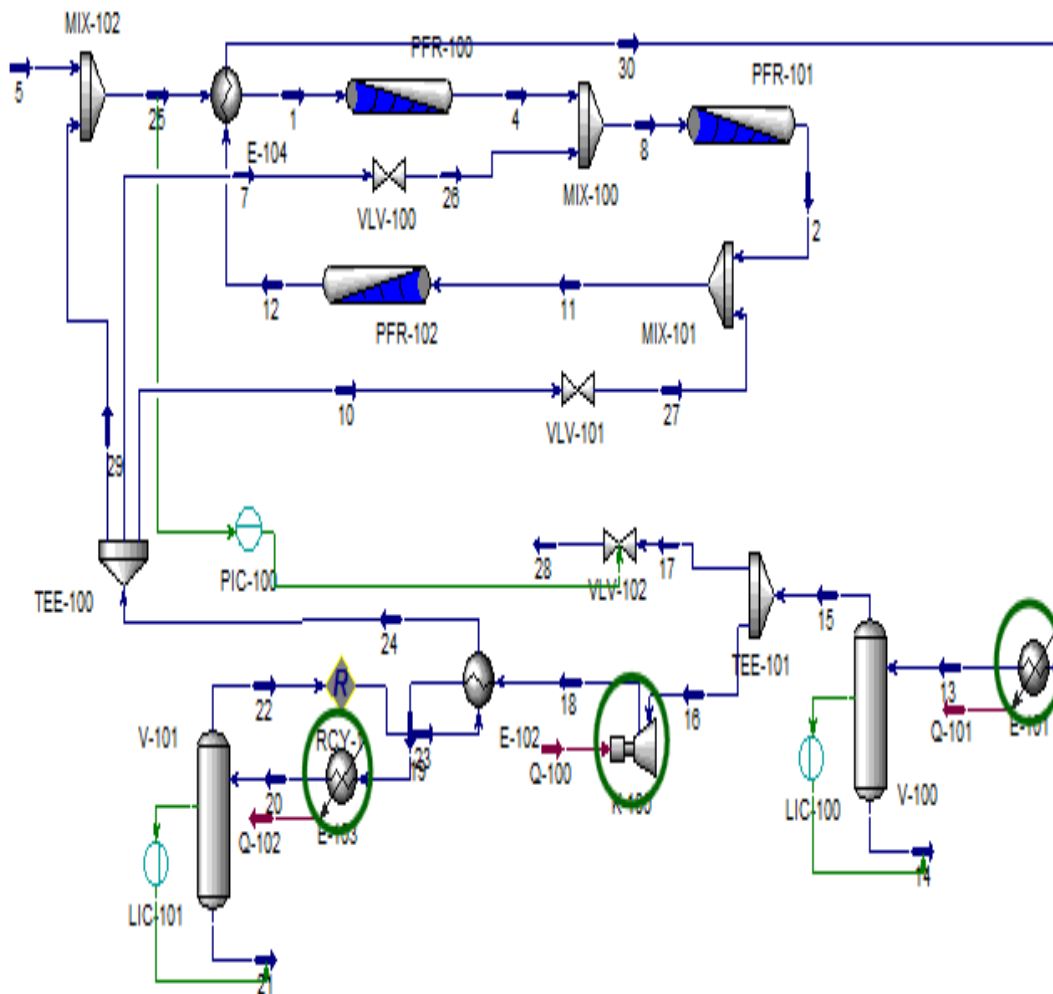


Figure 4.4: Determining the effect of steam to gas ratio using ratio 3.0,3.5,4.0

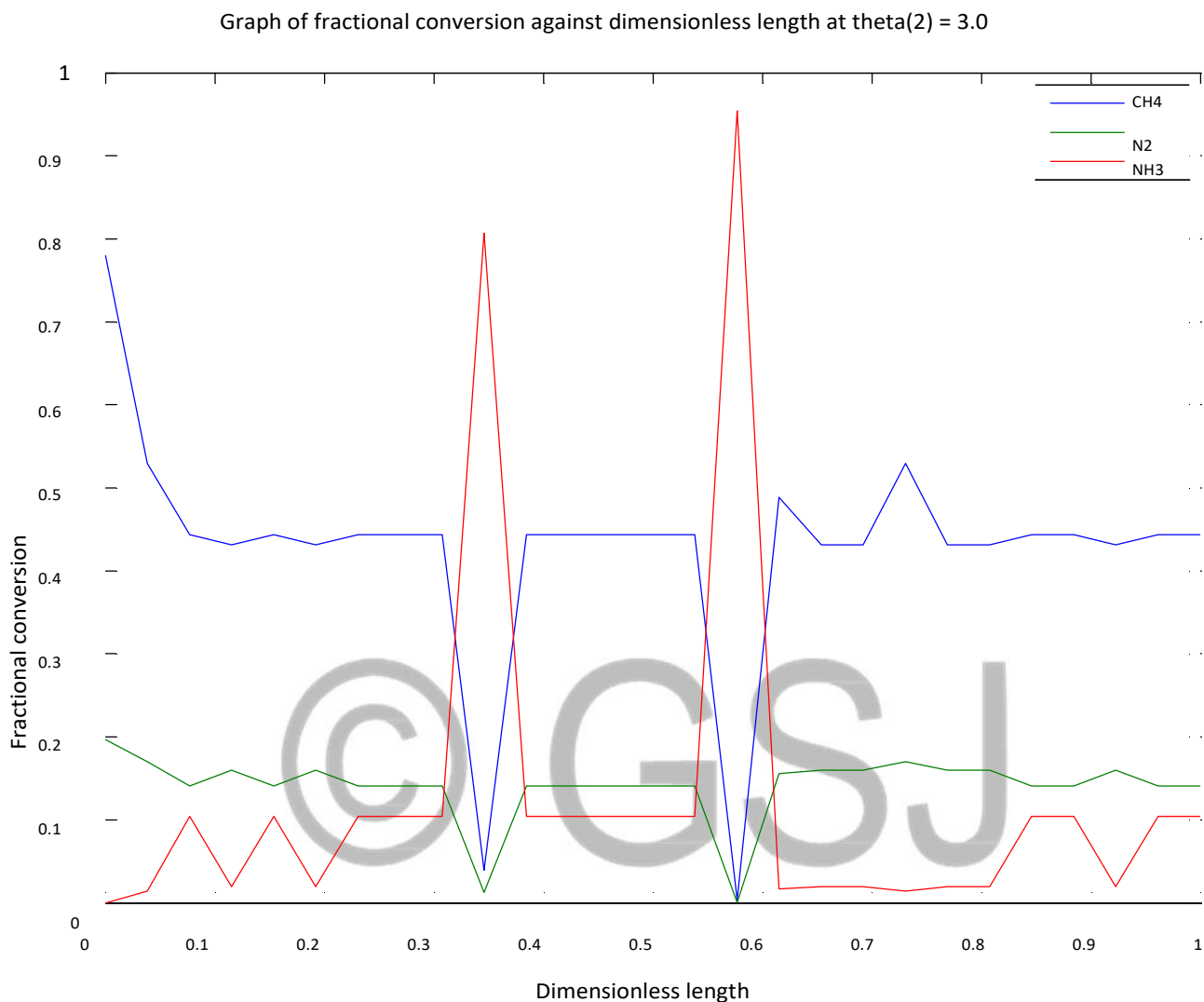


Figure 4.5: Fractional conversion against dimensionless reactor length for a steam to gas ratio of 3.0

Figure 4.5: illustrate the plot showing the effect of composition variation in the performance of ammonia production using steam to gas ratios.

This reaction is a reversible process and has backward and forward reaction (the yield of ammonia increases and the concentration of reactant of nitrogen and hydrogen decreases). Hence when the

backward reaction increases, the yield of ammonia decreases and the yield of nitrogen and hydrogen increases.

When the yield of ammonia reaches about 80% conversion, the yield of nitrogen and hydrogen drops to below 10%, hence when yield of nitrogen and hydrogen increases to about 15% and 45% conversion respectively, the yield of ammonia drops to about 10% conversion. Finally, when the yield of ammonia reaches at about 95% conversion, the yield of nitrogen and hydrogen drops to almost zero.

Conclusion

Conclusion

This research work on the effect of high steam to methane ratio in ammonia production involves review of literature, investigations, model development and matlab programming and simulation.

The following conclusion can be drawn from the work carried out;

- A mathematical model has been developed to investigate the effect of steam to gas ratio on the production of ammonia.
- A simulation to evaluate the effect of steam to gas ratio on the performance of ammonia was successfully carried out using MATLAB tool box and ASPEN hysys v8.6.
- An increase in the steam to gas ratio of 4.0 caused a corresponding increase in the conversion of methane, thereby favouring the performance of ammonia in the secondary reformer.
- The fractional conversion of methane gas was highest when the steam to gas ratio was 4.0
- Fractional conversion of nitrogen was constant in the reactor
- The highest conversion occurs in the inlet of the reactor.

REFERENCES

- AIChE. "2015 AIChE Salary Survey." *Chemical Engineering Progress* June 2015: 15-21.
- Akpa, J. G., & Raphael, N. R. (2014). Simulation of an Ammonia Synthesis Converter. *Canadian Journal of Pure and Applied Science*, 8, 2913-2923.
- Alkattib, A. M., & Boumaza, E. (2014). Simulation of the Performance of the Reforming of Methane in a Primary Reformer, World Academy of Science and Technology, *International Journal of Chemical and Molecular Engineering*, 8, 2.
- Almqvist, E. (2003). *History of Industrial Gases*. New York, NY: Kluwer Academic/Plenum, 83.
- Ball, J. (2015). Back to Basics: The Roles of N, P, K and Their Sourced. Jan. 2007. Web. 22 May 2015. <<http://www.noble.org/ag/soils/back2basics/>>.
- Catalano, J., Federico, G., Ivan, P., Mardilovich, N, K., Kazantzis, A., & Yi Hua, M. (2015). *Hydrogen Production in a Large Scale Water-Gas Shift Pd-Based Catalytic Membrane Reactor*. Worcester Polytechnic Institute, 21 Dec. 2011. Web. 2 Apr. 2015. <<http://pubs.acs.org/doi/abs/10.1021/ie2025008>>.
- Chavis, D., & Jason, C. (2014). The Effects and Uses of Ammonia in Agriculture. 4 June 2014. Web. 22 May 2015. <<http://www.brighthub.com/environment/science-environmental/articles/73262.aspx>>.
- Erisman, J. W., Mark, A., Sutton, Z. K., & Wilfried, W. (2015). How a Century of Ammonia Synthesis Changed the World. *Nature Geoscience*. 2008. Web. 17 May 2015. <<http://www.nature.com/ngeo/journal/v1/n10/full/ngeo325.html>>.
- Global Carbon Emissions. (2015). *CO2 Now*. 21 Sept. 2014. Web. 8 Aug. 2015. <<http://co2now.org/Current-CO2/CO2-Now/global-carbon-emissions.html>>.
- Himstedt, H., Alon, V., McCormick, U., & Edward L. C. (2013). *Small-Scale Production of Ammonia From a Combined Reactor-Membrane-Adsorber*. 8 Nov. 2013. Web. 24 May 2015. <<https://aiche.confex.com/aiche/2013/webprogram/Paper325135.html>>.
- Incitec Pivot Limited. *Louisiana Ammonia Plant*. Dyno Nobel, 17 Apr. 2013. Web. 4 Aug. 2015. <<http://www.asx.com.au/asxpdf/20130417/pdf/42f9brx9b4xscx.pdf>>.
- Overmann, O., & Stephen, R. (2011). Water Pollution by Agricultural Chemicals. Southeast Missouri State University, 2001. Web. 1 June 2015. <http://wps.prenhall.com/wps/media/objects/1027/1052055/Regional_Updates/update30.htm>.

- Perry, U., & Green, O. (2007). *Perry's Chemical Engineer's Handbook*, Eight Edition McGraw Hill professional
Process Flow Diagram of Ammonia Production. Retrieved 15/08/2019. from
<http://www.magicrot.ru/index.php?p=AmmoniaProduction&LANG_=ENG>.
- Roper, L., & David. S. (2015). *World Ammonia Production*. Retrieved 11/1/2019. from
<<http://www.roperld.com/science/minerals/ammonia.htm>>.
- Ruder, J., & Edwin, B. (2015). *Growing Demand for Fertilizer Keeps Prices High*. Retrieved
22/05/2019. from. <<http://www.bls.gov/opub/btn/volume-2/growing-demand-for-fertilizer-keeps-prices-high.htm>>.
- Schnitkey, G. (2014). Monthly Fertilizer Prices: Spring 2014 with Comparisons to 2009 through
2013." University of Illinois at Urbana-Champaign, Retrieved 15/05/2019. from
<<http://farmdocdaily.illinois.edu/2014/04/monthly-fertilizer-prices-spring2014-with-comparisons.html>>.
- Seider, S., Warren D., Seader, J. D., Daniel, R., Lewin, E., & Soemantri, W. (2010). *Product and
Process Design Principles: Synthesis, Analysis, and Evaluation*. Hoboken, New Jersey:
Wiley & Sons.
- Slack, A. V., & James, G. R. (2013). *Ammonia, Parts I, II, and III*, Marcel Dekker, New York.
- Smil, V. (2016). Detonator of the Population Explosion. Retrieved 22/05/2019. from
<<http://www.vaclavsmil.com/wp-content/uploads/docs/smil-article-1999-nature7.pdf>>.
- Thompson, S., Edward, V., & William, H. (2016). Ceckler. *Introduction to Chemical Engineering*.
New York, NY: McGraw-Hill.
- Thompson, S., Edward, V., & William, H., & Ceckler, D. (2012). *Introduction to Chemical
Engineering*. New York, NY: McGraw-Hill.
- U.S. Geological Survey, "Nitrogen (Fixed)—Ammonia Statistics,"
minerals.usgs.gov/minerals/pubs/historical-statistics/ds140-nitro.xlsx (Last Modified)
- United States. Environmental Protection Agency. *Inventory of U.S. Greenhouse Gas Emissions and
Sinks: 1990–2012*. Retrieved 23/01/2020 from <
<https://www.epa.gov/agl/agll/docs/barfinal.pdf> >.
- Van Der Ploeg, R. R., W. Bohm, and M. B. Kirkham. "History of Soil Science: On the Origin of the
Theory of Mineral Nutrition of Plants and the Law of the Minimum." Web. 17 May 2015.
http://academic.uprm.edu/dsotomayor/agro6505/VanderPloeg_etal_sssaj_Sprengel-Liebegpdf.pdf>.

Vorotto, A. (2015). PhD Raising the Standards: Enhanced Catalytic Performance for Global Ammonia Production." Quantumsphere. Web <http://qsinano.com/wp-content/uploads/2014/08/QSI-Ammonia-Whitepaper-FINAL-12-Aug-14.pdf>

Xu, J., & Froment, G.F. (1989). *American Institute of Chemical Engineering*, Methane Steam Reforming, Methanation and Water-Gas Shift: 1. Intrinsic Kinetics, 25, 88-103.

© GSJ